The effects of turbulence on the pressure distribution around a rectangular prism

Fred L. Haan Jr.[a,*], Ahsan Kareem[b], Albin A. Szewczyk[a]

[a] Department of Aerospace and Mechanical Engineering, University of Notre Dame, Notre Dame, IN 46556-5637, USA
[b] Department of Civil Engineering and Geological Sciences, University of Notre Dame, Notre Dame, IN 46556-5637, USA

Abstract

Pressure fields around a rectangular prism were studied using a new turbulence-generation technique. Employing jets blowing laterally to the main flow and stationary obstacles, the technique generates turbulent flows of varying scales. Results reported here constitute the first stage in a study of the effects of turbulence on the aeroelastic stability of long-span bridges. Past research in bridge stability has shown inconclusive results with respect to the scales of turbulence. Measurements were thus conducted in a host of flows holding the turbulence intensity constant while varying the integral scale. The integral scales of the incident flow had significant effects on the flow structure resulting in changes in the mean, rms, and negative peak pressure distributions. © 1998 Elsevier Science Ltd. All rights reserved.

1. Introduction

As an initial phase of a comprehensive study of the effects of turbulence on the aeroelastic stability of bridge decks, the present paper reports results of a study of the turbulence effects on the flow past a rectangular cylinder. The authors decided to approach the problem of scale effects by examining a flow pattern more basic than that around a bridge deck. A rectangular cylinder was chosen for this preliminary study in order to focus on basic flow physics rather than complex bridge geometries. Subsequent work will employ models of actual bridge decks. Wind-tunnel testing of bridge decks remains an integral component of long-span bridge design because of the complexity of the flow–structure interactions. At present, several contradictions exist

---

* Corresponding author.

in the bridge aerodynamics literature with respect to turbulence effects. While studying the flow phenomena involved with bridge deck aerodynamics, cues were taken from studies in general bluff-body aerodynamics.

This introduction discusses some contradictions in the literature and how they imply a dependence on the various scales of a turbulent flow. The approach followed by the authors – that of trying to identify the relative importance of the various scales – is then presented. The paper subsequently describes the turbulence generation techniques employed and briefly discusses some results.

Aeroelastic stability analyses of bridge decks often follow the empirical formulation of Scanlan and Tomko [1]. The aerodynamic derivatives, or "flutter derivatives", of this formulation capture some of the contradictions mentioned above. Different researchers using several different techniques have reported varying results when studying the effects of turbulence on bridge stability. Examining section model tests, we find the following. Huston [2] generated large integral scales by using flapping vanes and airfoils to generate gusting. His results showed a destabilizing trend, with respect to large-scale turbulence, in the flutter derivatives of certain section models. The results of Larose et al. [3], showed a stabilizing trend for turbulence, the opposite result of that of Huston. Further, the tests of Ref. [3] on their Storebaelt Bridge model – using forced vibration techniques with taut strip models – did not depend only on turbulence intensity. For similar turbulence intensities, grid-generated and boundary layer turbulent flows did not result in similar flutter derivatives. In fact, at turbulence intensities of $\sim 10\%$ some of the flutter derivatives were quite close to those for smooth flow.

Research using 3D aeroelastic models has mostly shown turbulence to have a stabilizing effect (see Ref. [4] for a brief summary). This has often been attributed to the lower spanwise correlation that turbulent flow has compared to uniform flow. Because of this stabilizing effect, smooth flow has often been considered a conservative test case.

In addition to experimental work, numerical stability analyses for bridge decks (see, e.g., Ref. [5]) have been performed using stochastic methods. The most common method of randomizing the equations of motion involves randomizing the dynamic pressure. This approach assumes that only the largest scales of turbulence have any effect on the aeroelastic forces. Smooth-flow flutter derivatives are used in many of these turbulence simulations thus assuming that the mechanisms for generating lift over the body are the same as for smooth flow cases.

In summary, changes in the energy content of different scales in a turbulent flow has been seen to alter the aerodynamic behavior of bridge decks. Turbulence intensity alone has been found to be insufficient to describe some of these changes. In addition, a fair amount of numerical work is done employing the assumption that small scale turbulence has negligible effects. It was determined, therefore, that scale effects deserve more attention.

The present work approached the effects of scales by first studying the pressure distributions about a stationary rectangular cylinder in a series of turbulent flow fields. This basic geometry allows one to focus on the effects of turbulence without the complications introduced by various bridge deck geometries. Existing research on the

pressure distributions around rectangular shapes is more plentiful than that for bridge deck pressure distributions making this a good starting point for the overall study. The work of Gartshore [6] and Bearman and Morel [7] showed the importance of free stream turbulence to the behavior of the separated shear layers. Enhanced mixing in the shear layers due to incident turbulence alters both their steady and unsteady behaviors. These alterations directly impact the pressure field. Pressure fields around bluff bodies with rectangular leading edges and long afterbodies – i.e. blunt flat plates – were the focus of Hillier and Cherry [8], Kiya and Sasaki [9], and Saathoff and Melbourne [10]. Their work showed that free stream turbulence contracts the separation bubble – resulting in steeper pressure recoveries. This contraction accompanies shifts in the mean, rms, and peak pressure distributions – their peaks have greater magnitudes and occur closer to the leading edge. These effects were found to increase with turbulence intensity and with integral scale.

Because most applications of these studies involve civil engineering structures immersed in atmospheric turbulence, one must consider appropriate turbulence intensities and scales. Long-span bridges can experience turbulence intensities as great as 20% and integral scales as large as ten times their deck width. This fact has led to work such as that of Nakamura and Ozono [11] to study how pressures are affected by much larger integral scales. Their research indicates that integral scale has little effect on mean pressure distributions until it is greater than twice the frontal dimension, D. Further increases in scale lead to mean pressures asymptotically approaching those of a smooth flow – suggesting that large-scale turbulence behaves like a flow of slowly varying velocity which can no longer significantly alter the mean flow structure. However, as Cherry et al. [12] and Kiya and Sasaki [9] have shown, the unsteady nature of the flow is highly complex and not fully explained by these mean values.

Li and Melbourne [13,14] have studied this unsteady structure in turbulent flow fields covering a range of intensities and scales. They generated desired turbulence parameter values using grids and by varying both the grid sizes and the distance behind the grids at which they placed their models. In addition, their work includes not only the blunt flat plate described above but also bodies of various finite afterbody lengths. Similar to Nakamura and Ozono [11], the behavior of mean pressure distribution reported in these studies showed a trend toward that of a smooth flow for integral scales greater than twice the frontal dimensions. Negative peak and rms pressures were found to increase with both turbulence intensity and scale up to a point where greater scales at a given intensity reversed this trend. Decreases in negative peak pressures with increasing scale seemed to occur near scales five times the frontal dimension (for all the afterbody lengths studied). Ref. [14] also reported that the effects of integral scales on all these distributions was intensified at greater turbulence intensities.

Integral scale effects do not completely describe the scales of a turbulent flow. Refs. [6,7] established that turbulence scales as small as the shear layer thickness significantly alter its behavior. Work by Tieleman and Akins [15] showed that pressure distributions depend more consistently on changes in the small-scale content of turbulent flows than on turbulence intensity. As will be discussed in the next section,

identifying the effects of scales while keeping the turbulence intensity constant is problematic. The results reported by Li and Melbourne [13,14] are difficult to characterize because as they increase the integral scale, the small-scale content decreases. Determining which scale change caused the measured pressure distribution changes is non-trivial.

The present setup stands as an alternative to the turbulence-generation techniques described above and represents an attempt to observe both small and large scales. Turbulence intensities of up to 20% and integral scales up to $7.8D$ were generated while small scale content was monitored. The model used had an aspect ratio similar to a common bridge deck (6.67 : 1).

2. Experimental setup

The atmospheric wind tunnel at the University of Notre Dame's Hessert Center for Aerospace Research was employed for the present study. Fig. 1 shows a top view of the facility. A 5 ft × 5 ft × 49 ft open-return test section is powered by a 30 hp motor. At a distance of 3.75 ft from the inlet, a plenum chamber pressurized by four fans surrounds the test section. Twelve rows of 23 holes in the walls of the test section form turbulence-generating jets lateral to the main flow. This jet apparatus is referred to as a "turbulence-generating box." An individual row's hole openings can be adjusted continuously from fully closed to fully opened allowing for a host of different configurations. This technique is based on the concepts of Betchov [16] and Lorenzen [17]. While a further description of the wind tunnel can be found in Refs. [18] and [19] describes the use of this tunnel for atmospheric boundary layer research.

Turbulent flow fields for the present work were generated using different arrangements of jets with varying exit velocities complemented by fixed obstacles. To alter the integral scales of the flow, six and twelve inch walls were mounted up or downstream of the box. Unfortunately, the complex nature of the system with its large number of tunable parameters does not show obvious patterns of continuous variations of the turbulence statistics. Rather, a number of different jet/obstacle combinations had to be run from which those arrangements that resulted in required parameter values were chosen.
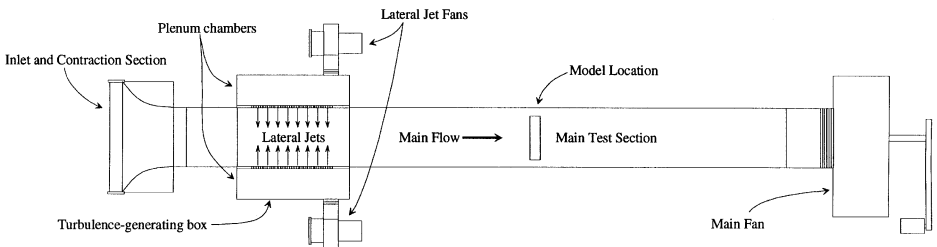

Fig. 1. Top view of the atmospheric wind tunnel showing the location of the turbulence-generating box.

The model consisted of a Plexiglas rectangular cylinder with dimensions 10 in × 1.5 in × 42 in (dimensions referred to as B, D, and L, respectively). The model was mounted 15 ft downstream of the turbulence-generating box. End plates of height $7D$ extended $2.5D$ and $5D$ from the model's leading and trailing edges, respectively.

An X-wire probe was used to measure the turbulent flow fields with the model absent. TSI's IFA-100 anemometer was used with data acquisition performed with two PCs – a Pentium-based system running a UEI WIN3016-PGSL data acquisition board and a 486-based system running a National Instruments AT-MIO-64F-5 data acquisition board. While future work will include traverses of a range of the flow field, the present paper reports only measurements made at the centerline of the test section. Pressure measurements were performed at 16 chordwise locations on the centerline of the model. Honeywell Microswitch 163PC transducers were mounted inside the model and connected to pressure taps with plastic tubing having an inner diameter of 0.050 in and a length of 7.0 in. Measurements were corrected for the dynamic effects of the tubing. Pressure transducers were sampled for 1000 s to arrive at the reported statistics.

3. Experimental results

3.1. Flow field measurement

After working through a number of different wind tunnel configurations, it was decided that two groups of flows would be examined. With the longitudinal turbulence intensities of these groups of flows relatively constant – $I_u = 14\%$ and $I_u = 20\%$ for groups 1 and 2, respectively – the scale effects can be observed. To quantify small scale content of these groups, the small-scale spectral density parameter of Teileman and Akins [15] (and earlier from Melbourne [20]) was used. This parameter is defined as

$$S_u = \frac{nS_{uu}(n)}{U} \times 10^6, \tag{1}$$

where U is the mean velocity and S_{uu}, the power spectral density function of the velocity fluctuations, is evaluated at frequency $n = aU/D$. This expression allows one to pick a frequency corresponding to wavenumbers near some fraction, a, of a typical body dimension, D. This parameter is basically a *scale-specific* turbulence intensity. All calculations of S_u in this paper take a to be 10 – resulting in a parameter that relates the energy of scales one tenth that of D. The parameters for these high intensity flows are listed in Tables 1 and 2. Reynolds number, Re, longitudinal turbulence intensity, I_u, vertical turbulence intensity, I_v, longitudinal integral scale, L_u, and the small-scale parameter, S_u, are reported. In what follows, longitudinal turbulence intensity and longitudinal integral scale will be referred to as turbulence intensity and integral scale, respectively. The range of control over the integral and fine scales was

Table 1
Turbulence parameters for flows with 14% longitudinal turbulence intensity

Flows with $I_u = 14\%$	Re	I_u	I_v	L_u	S_u
Smooth	10 700	1.1%	1.3%	–	–
Case 1	11 400	14.3%	14.5%	1.7D	5400
Case 2	10 900	14.5%	16.8%	2.3D	5000

Table 2
Turbulence parameters for flows with 20% longitudinal turbulence intensity

Flows with $I_u = 20\%$	Re	I_u	I_v	L_u	S_u
Smooth	10 700	1.1%	1.3%	–	–
Case 1	11 200	19.1%	17.5%	1.4D	16 000
Case 2	11 700	20.4%	16.9%	2.0D	15 000
Case 3	11 100	21.2%	16.9%	2.8D	13 000
Case 4	11 900	20.2%	14.8%	7.8D	9500

smaller than expected from this technique. With the technique still in development, greater control is anticipated in the future.

The goal for this study was to rely on the jets to provide a large inertial range and to control the small scale content while using obstacles to alter the integral scales. It was hoped that this approach would allow analysis of the differences in the effects of the largest scales (the integral scales) and the smallest scales in the flow. However, to maintain a nearly constant turbulence intensity, the total area under the power spectral density curve must remain constant. This requires that any increase of the large-scale content of a flow requires subsequent decrease in the small-scale content. Figs. 2 and 3 illustrate this tradeoff showing the power spectral density functions for the flows listed in the tables. Large inertial ranges for these flows are also evident from the plots.

3.2. Pressure measurements

The tradeoff between large and small scale content required to maintain constant turbulence intensity led to the authors to focus control efforts on the integral scale and then to observe the small scale content. In what follows, discussion centers around the integral scales keeping in mind that the effects of changes due to these scales cannot clearly be distinguished from those due to the accompanying small-scale changes.

For each group of flows listed in Tables 1 and 2, measurements were made of the distribution of pressure across the chord of the rectangular model. Figs. 4 and 5 show
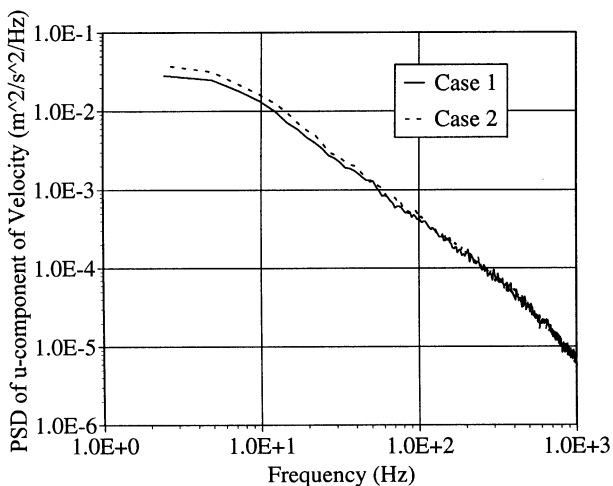
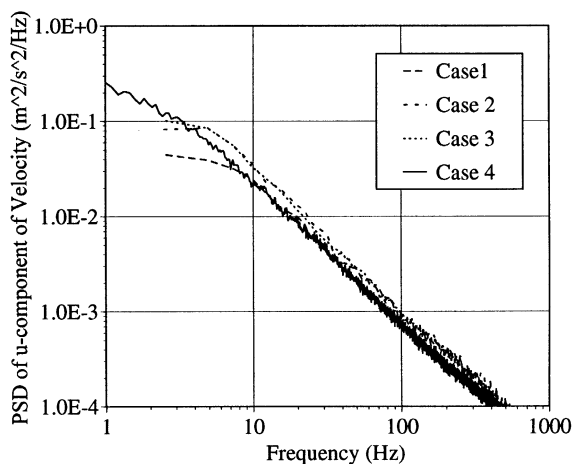Fig. 2. PSD of longitudinal component of velocity for the $I_u = 14\%$ cases.

Fig. 3. PSD of longitudinal component of velocity for the $I_u = 20\%$ cases.

the mean pressure distributions for the cases of 14% and 20% turbulence intensity, respectively. Higher turbulence intensities pull the peak of the pressure distribution closer to the leading edge. The slight difference in integral scale between the 14% cases does not result in significant mean value changes. The 20% cases show that as L_u increases (accompanied by the unavoidable decrease in S_u), the pressure recovery becomes steeper until $L_u = 2D$ where the trend reverses. With reference to the observations of Refs. [11,14] mentioned earlier, one may attribute this behavior to the
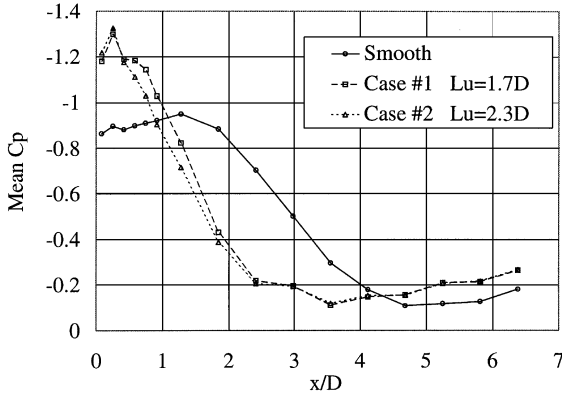
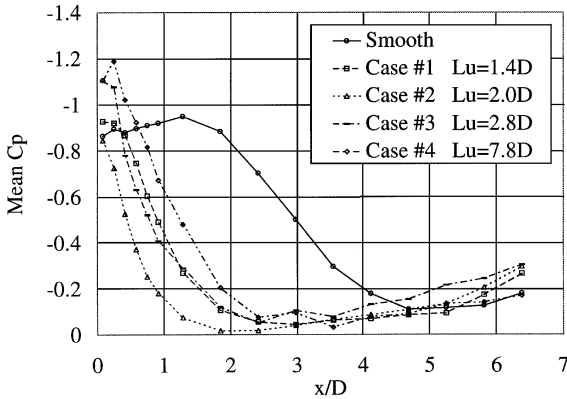Fig. 4. Mean pressure coefficient values for cases of $I_u = 14\%$.

Fig. 5. Mean pressure coefficient values for cases of $I_u = 20\%$.

fact that the shift of energy from the smaller to the larger scales result in a flow incapable of significantly altering the shear layers. This flow, with less small-scale content (note the decrease of S_u in Table 2) to alter the shear layer behavior is more like one of slowly varying velocity – i.e. a smooth flow. The peak of the rms distribution, however, continues to increase as L_u increases which is not consistent with a trend toward a smooth-flow distribution.

Figs. 6 and 7 show the rms values of the pressure coefficients for the 14% and 20% groups, respectively. As observed in Refs. [8–10,13,14], greater turbulence intensity draws the peaks of the distributions closer to the leading edge. The actual values measured were up to 80% greater than those for Li and Melbourne's [14] finite afterbody cases (models of $H/D = 4$ in flows with 11% turbulence intensity). For the 14% cases of Fig. 6, a slight increase in L_u increases the rms values and shifts the
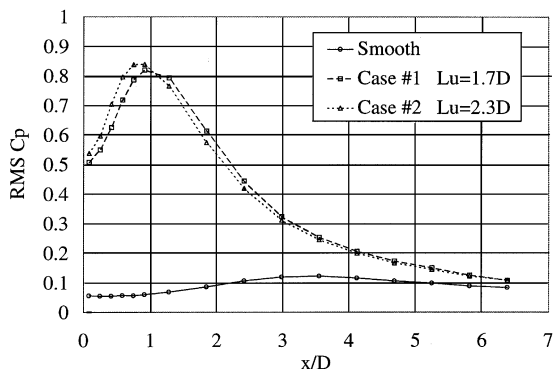
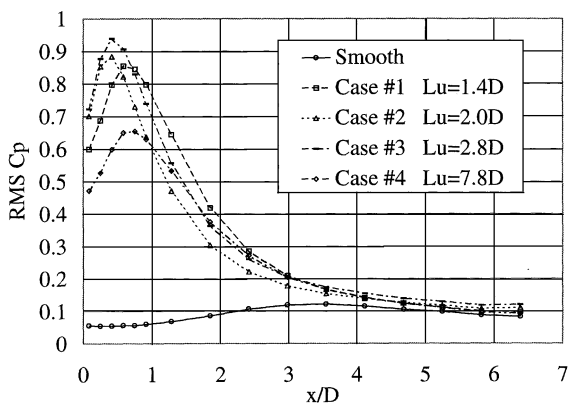Fig. 6. RMS values of pressure coefficients for cases of $I_u = 14\%$.

Fig. 7. RMS values of pressure coefficients for cases of $I_u = 20\%$.

distribution forward. Increasing L_u from 1.4D to 2.8D for the 20% case follows this same trend with the highest rms values occurring for $L_u = 2.8D$ and $S_u = 13\,000$. Larger integral scales, however, reverse this trend back toward a distribution more like that of a smooth flow. While this phenomenon was reported in reference [14] for models with very long afterbodies, such a reversal was not observed for models with a finite afterbody length (up to $H/D = 4$ where H is the afterbody length) for integral scales up to 6.71D.

Peak values of pressure coefficients for the 14% and 20% groups are plotted in Figs. 8 and 9, respectively. The magnitudes of the peaks for the slightly different integral scales of the 14% group were quite similar until $x/D = 0.6$ beyond which lower values occurred for the greater integral scale. Negative peak distributions for the 20% group showed that the highest peak values occurred for an L_u of 1.4. Case 4 of the 20% group was the closest of the group to smooth flow values. This trend with
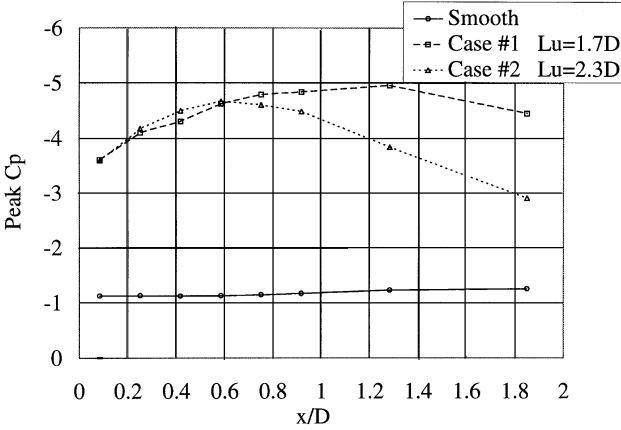
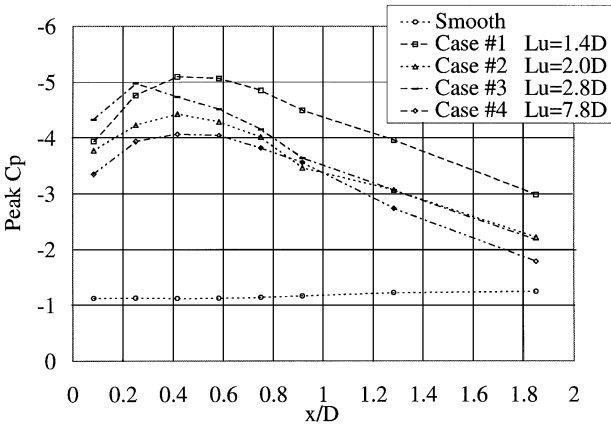Fig. 8. Peak values of pressure coefficients for cases of $I_u = 14\%$.

Fig. 9. Peak values of pressure coefficients for cases of $I_u = 20\%$.

increasing L_u values follows that seen with the rms values. Li and Melbourne [14] observed a integral scale beyond which negative peak values decreased. Their data showed this critical value to be near $L_u = 5D$ while the present data set can specify a value in the range of $2.8D$ to $7.8D$.

4. Conclusions

Pressure distributions measured on a rectangular cylinder in flows of constant turbulence intensity and varying scales have shown that scales do have significant

effects on the flow structure. Up to a critical value, increases of integral scale, with the attendant decreases in small-scale content necessary to maintain constant turbulence intensity, altered mean, rms, and negative peak pressure distributions. With increasing integral scale, the peaks of these distributions moved closer to the leading edge and the shapes of the distributions grew narrower on either side of the peaks. Integral scales above some critical value between $2.8D$ and $7.8D$ resulted in flows with pressures distributions trending back toward the results of smooth flow tests.

Illuminating the *relative* effects of small and large scales will require a different nature of tests than those presented here. The turbulence-generation technique described here offers a unique way to vary the relevant statistics. Future work will include more configurations of the facility for a greater number of individual scale variations – greater control over parameters coming from further experience with the technique. Subsequent studies will include streamwise and spanwise pressure correlations, simultaneous pressure and velocity measurements, and dynamic testing to observe the turbulent scale effects on flutter derivatives.

Acknowledgements

References

[1] R.H. Scanlan, J.J. Tomko, Airfoil and bridge deck flutter derivatives, J. Eng. Mech. Div. ASCE 97 (6) (1971) 1717–1737.

[2] D.R. Huston, The effects of upstream gusting on the aeroelastic behavior of long suspended-span bridges, Dissertation, Department of Civil Engineering, Princeton University, 1986.

[3] G.L. Larose, A.G. Davenport, J.P.C. King, On the unsteady aerodynamic forces on a bridge deck in turbulent boundary layer flow, Proc. 7th US Nat. Conf. on Wind Engineering, UCLA, 1993.

[4] R.H. Scanlan, N.P. Jones, Aeroelastic analysis of cable-stayed bridges, J. Struct. Eng. 116 (2) (1990) 279–297.

[5] C.G. Bucher, Y.K. Lin, Stochastic stability of bridges considering coupled modes, J. Eng. Mech. 114 (12) (1988) 2055–2071.

[6] I.S. Gartshore, The effects of free stream turbulence on the drag of rectangular two-dimensional prisms, Boundary Layer Wind Tunnel Laboratory 4-73, The University of Western Ontario, 1973.

[7] P.W. Bearman, T. Morel, Effect of free stream turbulence on the flow around bluff bodies, Prog. Aerospace Sci. 20 (1983) 97–123.

[8] R. Hillier, N.J. Cherry, The effects of stream turbulence on separation bubbles, J. Wind Eng. Ind. Aerodyn. 6 (1981) 49–58.

[9] M. Kiya, K. Sasaki, Free-stream turbulence effects on a separation bubble, J. Wind Eng. Ind. Aerodyn. 14 (1983) 375–386.

[10] P.J. Saathoff, W.H. Melbourne, The generation of peak pressures in separated/reattaching flows, J. Wind Eng. Ind. Aerodyn. 32 (1989) 121–134.

[11] Y. Nakamura, S. Ozono, The effects of turbulence on a separating and reattaching flow, J. Fluid Mech. 178 (1987) 477–490.

[12] N.J. Cherry, R. Hillier, M.E.M.P. Latour, Unsteady measurements in a separated and reattaching flow, J. Fluid Mech. 144 (1984) 13–46.

[13] Q.S. Li, W.H. Melbourne, An experimental investigation of the effects of free-stream turbulence on streamwise surface pressures in separated and reattaching flows, J. Wind Eng. Ind. Aerodyn. 54/55 (1995) 313–323.

[14] Q.S. Li, W.H. Melbourne, Effects of turbulence on surface pressures of a flat plate and rectangular cylinders in separated and reattaching flows, Papers for the 9th Int. Conf. on Wind Engineering, vol. 1, Wiley Eastern Limited, New Delhi, 1995.

[15] H.W. Tieleman, R.E. Akins, Effects of incident turbulence on pressure distributions on rectangular prisms, J. Wind Eng. Ind. Aerodyn. 36 (1990) 579–588.

[16] R. Betchov, On the fine structure of turbulent flows, J. Fluid Mech. 3 (1957) 205–216.

[17] C.J. Lorenzen, An experimental investigation of the structure of high intensity turbulence, Dissertation, Department of Aerospace and Mechanical Engineering, University of Notre Dame, 1972.

[18] F.L. Haan, Jr., A. Kareem, A.A. Szewczyk, The University of Notre Dame atmospheric wind tunnel, Proc. 10th Engineering Mechanics Specialty Conf., ASCE, Boulder, CO, 1995.

[19] V.W. Nee, B. Cheung, V. Liu, A.A. Szewczyk, K.T. Yang, Simulation of the atmospheric surface layer, Proc. 3rd U.S. Natl. Conf. on Wind Engineering, Research 5 (1978) 1–8.

[20] W.H. Melbourne, Turbulence effects on maximum surface pressures – a mechanism and possibility of reduction, Proc. 4th Int. Conf. on Wind Effects on Buildings and Structures, Cambridge University Press, Cambridge, 1979, pp. 541–551.